metals

MDPI

Article

Reactions and Morphologies of Mg and Mg/Teflon/Viton Particles during Oxidation

Yifan Li [1], Jie Wang [1], Dong Shen [2], Haoying Liu [1], Dongming Song [1] and Yanchun Li [1,*]

[1] Department of Chemical Engineering, Nanjing University of Science and Technology, Nanjing 210097, China
[2] Zhejiang Material Industry Guanghua Civil Explosive Materials Co., Ltd., Hangzhou 310008, China
* Correspondence: liyanchun@njust.edu.cn; Tel.: +86-13601457975

Abstract: A thorough investigation on the reactions and morphologies of Mg particles and Mg/Teflon/Viton (MTV) during oxidation were conducted via thermal gravity-differential scanning calorimetry (TG-DSC) and scanning electronic microscopy. The results showed that the oxidation of Mg is fast. It merely changed the metallic luster of Mg before 550 °C, and only a few particles changed to a white irregular shape at 600 °C. However, all of the Mg particles oxidized to porous irregular shaped MgO at 650 °C. Herein, the oxidation of Mg particles ended by its melting point, and the whole process is a solid–gas-phase reaction. On the other hand, when MTV reacted in air, the reaction could be divided into two stages: the fluorination of Mg and the oxidation of the exceeded Mg. In the first stage, a dense MgF_2 shell was formed by the solid–solid fluorination. The dense MgF_2 shell could impede the oxidation of Mg. As a result, the oxidation of Mg began after its melting. Furthermore, liquid Mg could vaporize at higher temperature, which could burst out from the MgF_2 shell and react with oxygen. The MgF_2 shell exhibited a dense feature, not only protecting the Mg particles from the heterogeneous oxidation at lower temperature, but also facilitates the homogeneous oxidation at higher temperature.

Keywords: Mg particles; MTV; TG-DSC; SEM; EDS

Citation: Li, Y.; Wang, J.; Shen, D.; Liu, H.; Song, D.; Li, Y. Reactions and Morphologies of Mg and Mg/Teflon/Viton Particles during Oxidation. *Metals* **2023**, *13*, 417. https://doi.org/10.3390/met13020417

Academic Editors: Kristián Máthis and Dmytro Orlov

Received: 11 January 2023
Revised: 9 February 2023
Accepted: 14 February 2023
Published: 17 February 2023

1. Introduction

Magnesium, due to its low melting and boiling points and easy ignition, reacts readily with oxidizers, making it a highly reactive metallic fuel. This characteristic makes it a useful component in various industrial and pyrotechnic applications including ignition charge, pyrotechnic, decoy, and water-based propellent.

When magnesium reacts with an oxidizer, it undergoes a rapid and exothermic combustion reaction that forms a high-temperature combustion zone at the core of the magnesium particle. This reaction generates a mixture of multi-phase products including condensed particles and high-temperature gases. In 1954, Coffin conducted a study on the combustion of magnesium and discovered that the reaction primarily took place in the gas phase, instead of on the surface as previously believed [1]. George and his colleagues used the Polanyi dilute-diffusion-flame method to study the Mg-O_2 system and concluded that the majority of oxidation occurs as a heterogeneous reaction on the growing magnesium oxide (MgO) particles [2]. E.S. Ozerov [3] investigated the combustion of Mg in a hybrid gas of O_2, Ar, and N_2, and proposed surface ignition and vapor-phase ignition. Guillaume Moser [4] calculated the kinetics of the slow oxidation of Mg particles in diameters of 20–50 μm and 50–71 μm. The results suggest that the slow oxidation of Mg can be divided into two steps: slow oxidation and rapid oxidation. E. Ya. Shafirovich [5] discovered that when Mg combusted in CO and CO_2, the slow oxidation occurred by the temperature of 700 °C, and then transferred to slow heterogeneous combustion. Numerous investigations on the combustion mechanism have been reported including heterogeneous oxidations, various reaction atmosphere, reaction kinetics, and combustion morphology, where slow

oxidation has been reported as the first step of the combustion of Mg. However, the research on the slow oxidation of Mg has not been thoroughly investigated. Currently, the focus of the slow oxidation of Mg is mainly on the oxidation kinetics, the activity of Mg after slow oxidation, and the macro-morphology of Mg after slow oxidation [4,6–8]. The micro-morphology on the reaction surface of Mg where the slow oxidation occurs has not been thoroughly investigated.

Fluorine, the most electronegative element, has been utilized in energetic materials. Not only can it be applied as an oxidizer to thermite and pyrotechnics with metal and non-metal inorganics, it can also be used as an energetic additive to enhance the activity of the fuel. The reason for the enhanced activity is mainly because fluorine can react with the oxidation layer of the fuel, leading to the active core of the fuel being exposed to the oxidizer. However, the activity of Mg after fluorination has rarely been investigated. Furthermore, the defects in MgO could be influenced by various environmental conditions. G. Baubekova et al. thoroughly investigated the defects in MgO under different irradiation conditions [9]. The results showed that the experimental activation energy for interstitial migration is much smaller than that of a perfect MgO crystal. This could be due to the specific spatial distribution of radiation induced F-type centers and complementary interstitial oxygens. Meanwhile, the defects in MgF_2 could also be influenced by the environment. A.I. Popov et al. investigated the defects in MgF_2 induced by neutrons [10], and the scintillation property of MgF_2 was also investigated [11]. These suggest that when fluorine co-exists in the oxidizing environment, the morphology of MgO might also change. On the other hand, Seied [12] used the solvent–nonsolvent technique to coat Viton on the Mg particles, discovering the poor oxidation property of coated Mg. Li et al. [13] reported that in the composite of Mg/Teflon/Viton (MTV), the exceeded Mg could be oxidized at a higher temperature after its fluorination.

To gain a comprehensive understanding of the reactions and morphologies of both magnesium particles and magnesium/Teflon/Viton (MTV) during oxidation, a series of experiments were conducted. First, the oxidation of magnesium particles at different heating rates to analyze the reaction process were investigated. Additionally, ex situ macro-micro morphological analysis of the oxidation process using an optical microscope and scanning electron microscope were conducted. The oxidation of the MTV compound at different heating rates and a similar morphological analysis of the compound's reaction with air were both performed. Based on these findings, the researchers proposed a mechanism for the prolonged oxidation process of magnesium.

2. Experiments

2.1. Sample Preparation

Mg spherical particles (100~250 mesh) were obtained from Tangshan Weihao Magnesium Powder Co. Ltd. (Tangshan, Henan, China). The Mg/Teflon/Viton sample was prepared by the following procedure: 0.5 g of Viton was first cut into 1 mm cubes, and dissolved in 2 mL acetone. Then, 5.00 g Mg was physically mixed thoroughly with 5.00 g Teflon powder (5 μm, Meryer, Mw = 100.015). The Mg/Teflon mixture was added into the Viton solution. Then, the ternary mixture was stirred fiercely until almost all of the solvent was vaporized. Later, the mixture was sorted through a 30-mesh screen. The Mg/Teflon/Viton (MTV) grain was later dried at the temperature of 60 °C for 2 h. Finally, the MTV grain was sorted again through a 30-mesh screen, and the sample on the screen was gathered to be tested.

2.2. TG/DSC Experimental Procedure

TG/DSC were performed simultaneously in Mettler-Toledo TG/DSC 3+. A 0.7 mg sample was loaded into a 40 μL Al_2O_3 crucible inside the apparatus and programmed to be heated from 30 to 1200 °C at the heating rate of 10 K/min. The protective gas flow was programmed as high purity argon of 20 mL/min, and the active gas flow was programmed

as high purity O_2 of 20 mL/min. To the complete contact of the sample with oxygen, the lid to the assorted crucible was not applied.

2.3. The Morphology Characteristic on the Oxidation Products of Mg

2.3.1. The Preparation of the Oxidation Products of Mg

To obtain the oxidation product of Mg, Mg spherical particles were heated in in Mettler-Toledo TG/DSC 3+. The sample of 0.5~1 mg Mg was heated to 500, 550, 600, 650, 700 °C at the heating rate of 10 K/min in the TG-DSC apparatus under high purity oxygen at the flow rate of 20 mL/min, respectively.

On the other hand, to obtain the oxidation product of Mg in MTV, the MTV grain was heated in a Mettler-Toledo TG/DSC 3+. A sample of 1.0~2.0 mg MTV (single grain) was heated to 500, 600, 700, 800, and 900 °C under the same configuration of the heating rate and gas flow. To thoroughly react with oxygen, the lid of the assorted crucible was not applied.

2.3.2. The Morphology of the Oxidation Products of Mg Characterized via Optical Microscopy

After heating in the TG/DSC apparatus, the oxidation product, along with the Al_2O_3 crucible, was set on the sample platform of the HiROX Digital Microscope KH-7700 (HiROX, Tokyo, Japan). The lens of KH-7700 was MX-5040RZ (magnification: 50~400 times, HiROX, Tokyo, Japan) with an adaptor of AD-5040HS (HiROX, Tokyo, Japan). The focal length was adjusted by a HiROX CT-7 motor controller. The white balance was set as AUTO, and the capturing model was STILL IMAGE. The magnification was set as 50, 100, 200, and 300 times, respectively.

2.3.3. The Morphology of the Oxidation Products of Mg Characterized via SEM-EDS-Mapping

After the characteristics were obtained via optical microscopy, the oxidation product of Mg was gathered from the crucible and characterized by a scanning electron microscope (SEM, FEI Quanta 400FEG, Hillsboro, OR, USA 20 kV). Energy dispersive X-ray spectroscopy (EDX, EDAX APPLO X1, EDAX Inc., Mahwah, NJ, USA) was used to further discern the compositional detail.

3. Results and Discussion

3.1. TG/DSC Results of the Oxidation of Mg

To investigate the oxidation progress of Mg, it was first heated in a Mettler-Toledo TG/DSC 3+ from 30 to 1200 °C under an O_2 atmosphere at the heating rate of 5, 10, 15, 20, 25, and 30 K/min, respectively. The results are depicted in Figure 1.

As shown in Figure 1a, the thermogravimetric (TG) curve showed a 4.7% increase in mass from 400 to 550 °C when heated at 5 K/min, while the curve at 10 K/min showed a 2.3% increase. From 400 to 619 °C, the mass increase was 17.7% at 5 K/min and 5.6% and 1.5% at 10 and 15 K/min, respectively, as shown in Figure 1c. However, no exothermic peak was observed on the related differential scanning calorimetry (DSC) curves during the temperature range of 400 to 619 °C, as shown in Figure 1b. This suggests that the gas–solid-phase oxidation of magnesium occurred at the low temperature of 400 °C. This stage is known as slow oxidation, and involves the formation of magnesium oxide (MgO) nuclei on the surface. The growth of these nuclei was related to a nucleation mechanism and modeled using a first-order Mampel reaction function [7].

Additionally, the main increase in mass between 620 °C and 650 °C was due to the main oxidation of magnesium. During this time, the mass increased from 40.9% (at 5 K/min) to 65.2% (at 30 K/min), as evidenced by several exothermic peaks on the related DSC curve shown in Figure 1c,d. At this stage, the Avrami–Erofeev reaction function was used to model the reaction, and the order of the reaction function can vary depending on the particle size [6].

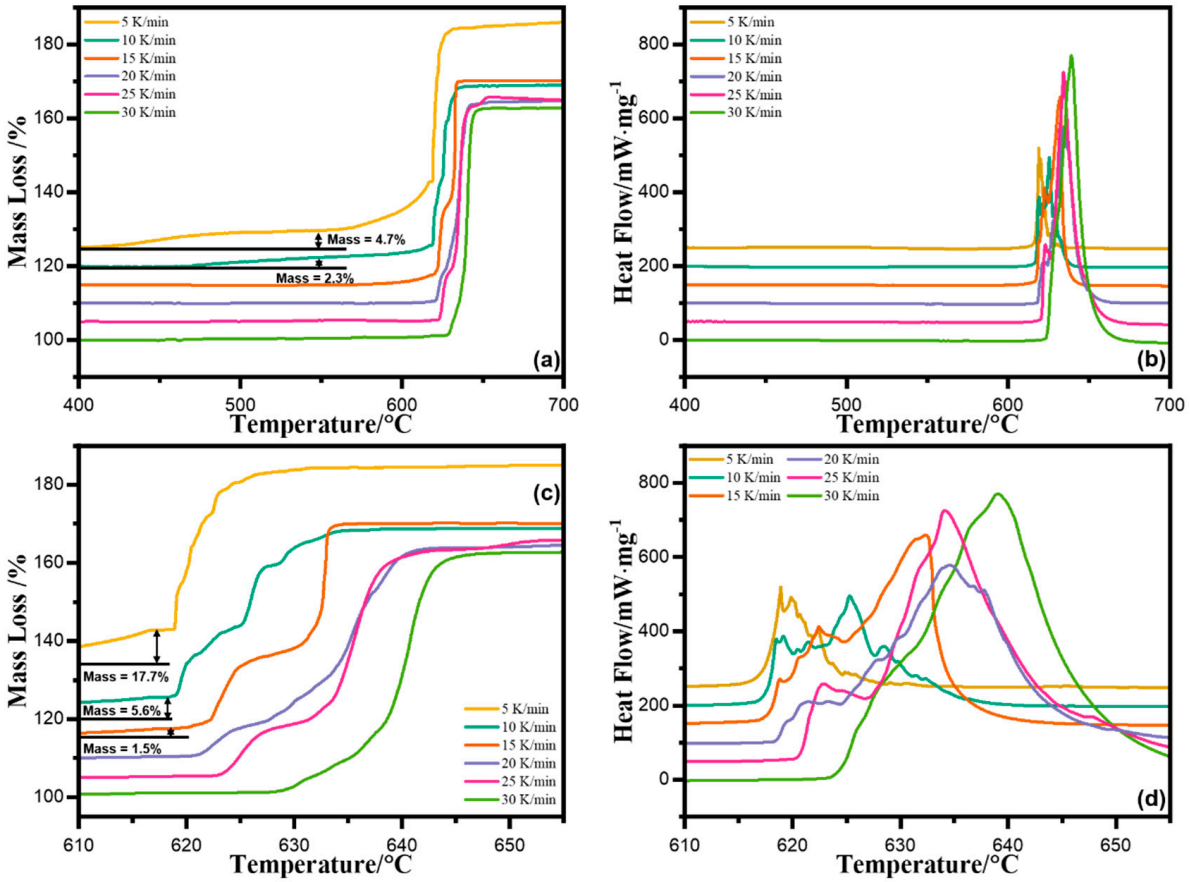

Figure 1. The TG-DSC curves of the oxidation of Mg at 5, 10, 15, 20, 25, and 30 K/min under the atmosphere of O_2. (**a**,**b**) Curves of TG and DSC from 400~700 °C, respectively; (**c**,**d**) curves of TG and DSC from 610~660 °C of TG and DSC, respectively. The theoretical mass increase of the oxidation of Mg is 66.7%.

3.2. The Morphology of the Oxidation Products of Mg Characterized via Optical Microscope

To generally investigate the ex situ morphology of spherical Mg particles under different oxidation temperatures, Mg was heated at 500, 550, 600, 650, 700, and 1200 °C, and the products were characterized via an optical microscope. The results are shown in Figure 2.

The results of the oxidation of the Mg particles as shown in Figure 2 demonstrate that the product can be divided into two morphologies: spherical particles with metallic luster and white particles with irregular shapes. At 600 °C, the spherical particles retained their metallic luster, while some of them changed to an irregular shape without luster. As the temperature rose above 600 °C, all of the particles transformed into white and irregular-shaped particles.

The data in Figure 1a indicate that the oxidation of Mg at a heating rate of 10 K/min began at 475 °C and the main mass increase occurred at 618 °C. Correspondingly, the majority of the Mg particles remained spherical with metallic luster at 600 °C, indicating that the slow oxidation did not significantly alter their morphology. However, as the rapid oxidation started, the morphology of the Mg particles changed as they were completely oxidized to MgO. Previous studies by V.I. Shevtsov [14] have shown that Mg particles can grow up to two or three times their initial size due to the presence of hydrogen. However, in this case, the expansion of Mg was less than two times.

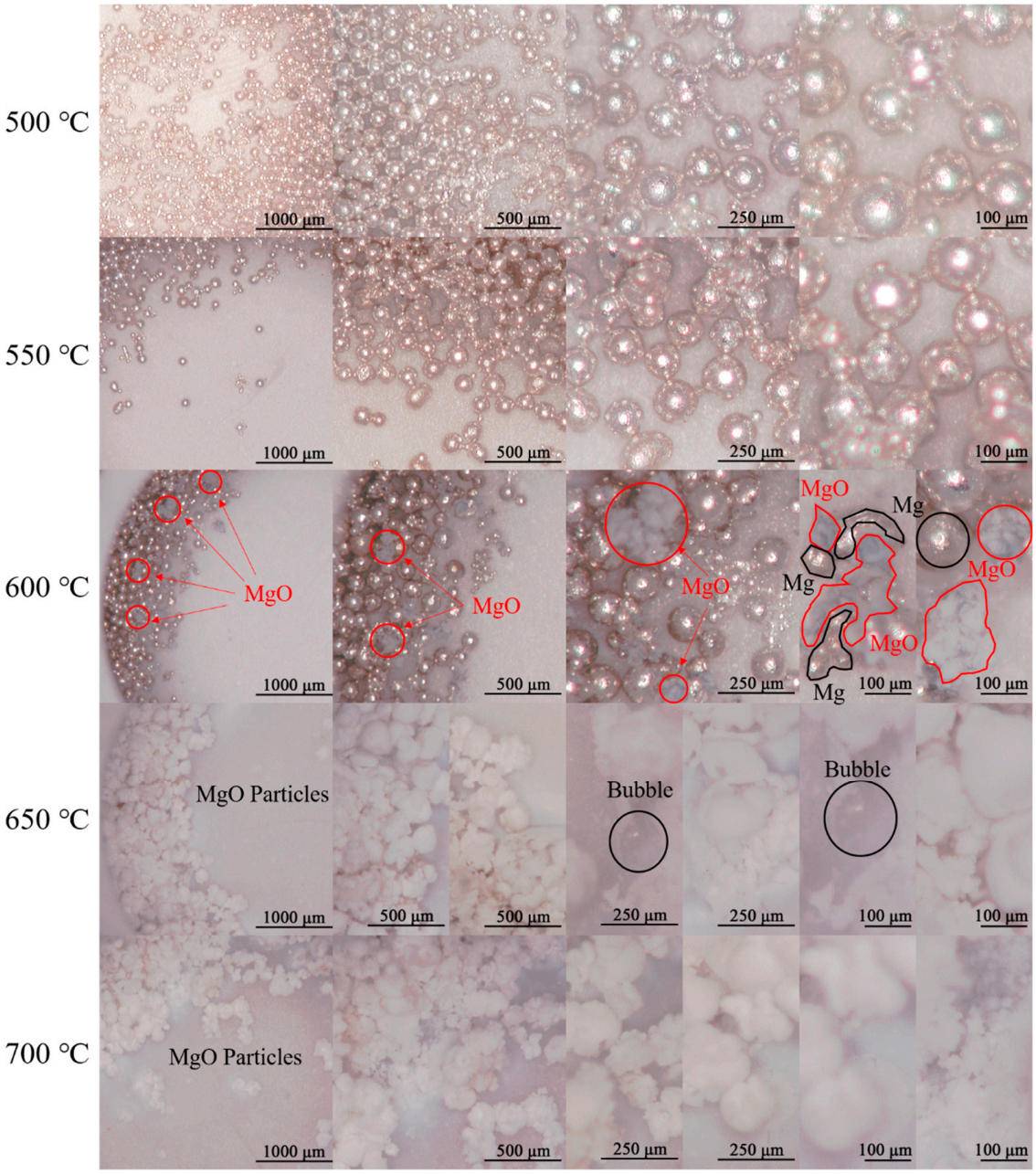

Figure 2. The morphology of the residues of the oxidation of Mg at 500 °C, 550 °C, 600 °C, 650 °C, and 700 °C magnified 50, 100, 200, and 300 times via an optical microscope. The white balance was set to AUTO.

3.3. The Morphology of the Oxidation Products of Mg Characterized via SEM-EDS Mapping

To thoroughly investigate the morphology of the oxidation products of Mg, SEM-EDS mapping was conducted on the same samples in Section 3.2. The results are shown in Figure 3.

As shown in Figure 3a, during the heating process from 25 to 600 °C, the surface of the spherical Mg particles displayed the growth and spread of MgO nodes. At temperatures of 650 and 700 °C, no spherical particles were visible. The growth of these nodes can be attributed to the slow oxidation stage, which involves the formation of MgO nuclei on the surface.

To eliminate experimental error, the SEM magnification was reduced, and the results are displayed in Figure 3b. At 600 °C, the morphologies of A2 and A4 were still spherical,

similar to those at 500 °C. Meanwhile, A1 and A3 showed irregular shapes, which were similar to those at 650 °C (A5) and 700 °C (A6). Notably, the particle in the center of the figure at 600 °C showed two morphologies divided by C1. The EDX results (wt%) in A1 to A4 are summarized in Table 1 to provide insights into the changes in the content of Mg and O on the particle surfaces.

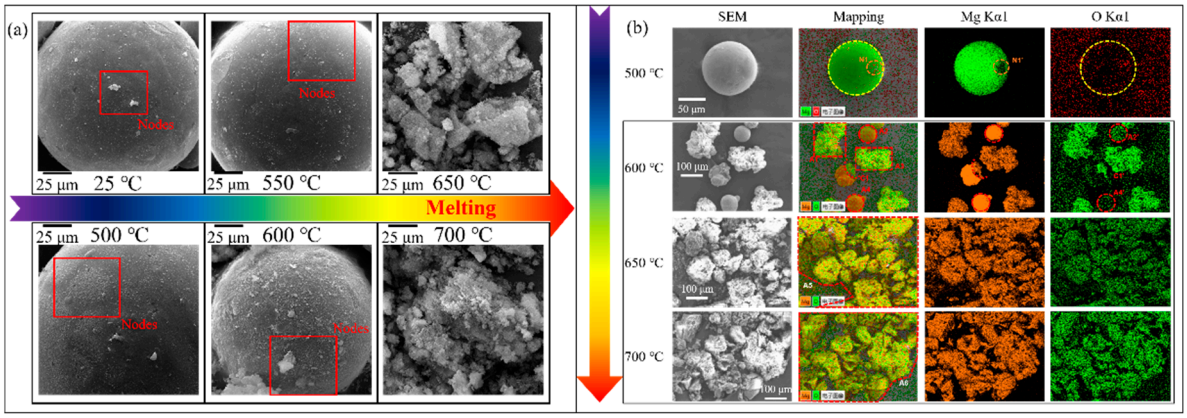

Figure 3. (**a**) The morphology of the surface of Mg after heating at 500 °C, 550 °C, 600 °C, 650 °C, and 700 °C under O_2. The heating rate was 10 K/min. The magnification was 5000 times. (**b**) The mapping results of the surface of Mg after heating at 500 °C, 600 °C, 650 °C, and 700 °C under O_2. The heating rate was 10 K/min. The magnification included 2500 and 5000 times. Detailed EDS-SEM results are depicted in Figures S1–S8.

Table 1. The EDX results (wt%) of the Mg spherical particles after heating at 600, 650, and 700 °C. Theoretically, the mass ratio of MgO is 60:40.

Temperature	Element	Mg	O
600 °C	A1	57.7	42.3
	A2	83.7	16.3
	A3	56.46	43.54
	A4	94.42	5.58
650 °C	A5	59.9	40.1
700 °C	A6	60.76	39.24

As shown in Table 1, the ratio of Mg to O in A1 and A3 was around 60:40, indicating the full oxidation of these particles. On the other hand, the ratio of Mg to O in A2 and A4 was far from the theoretical ratio, suggesting an incomplete oxidation of Mg. After being heated at 650 and 700 °C, the ratio of Mg to O in A5 and A6 was close to 60:40, indicating complete oxidation. These EDX results suggest that the complete oxidation product of Mg, MgO, had an irregular shape, while the intermediate oxidation product still had a spherical shape.

These findings confirmed that at 600 °C, the oxidation of Mg began, but did not change the spherical shape and metallic luster. At the same time, some of the particles were fully oxidized and changed to an irregular shape, while the others remained unchanged. However, as the temperature rose to 650 °C and higher, all particles were fully oxidized to MgO and had a white, irregular shape.

In conclusion, the oxidation of Mg is fast and only affected the morphology of Mg before 550 °C. At 600 °C, only some of the Mg particles changed to a white, irregular shape, and all Mg particles were fully oxidized to MgO at 650 °C.

3.4. TG/DSC Results of the Oxidation of MTV in Air

To investigate the oxidation of Mg in a fluorinated atmosphere, the MTV sample was heated from 30 to 1200 °C under the atmosphere of O_2, at the heating rate of 5, 10, 15, 20,

25, and 30 K/min, respectively. The results are depicted in Figure 4. Due to the minimum addition of Viton (wt% = 4.8%), the effect of it on the reactions was neglected.

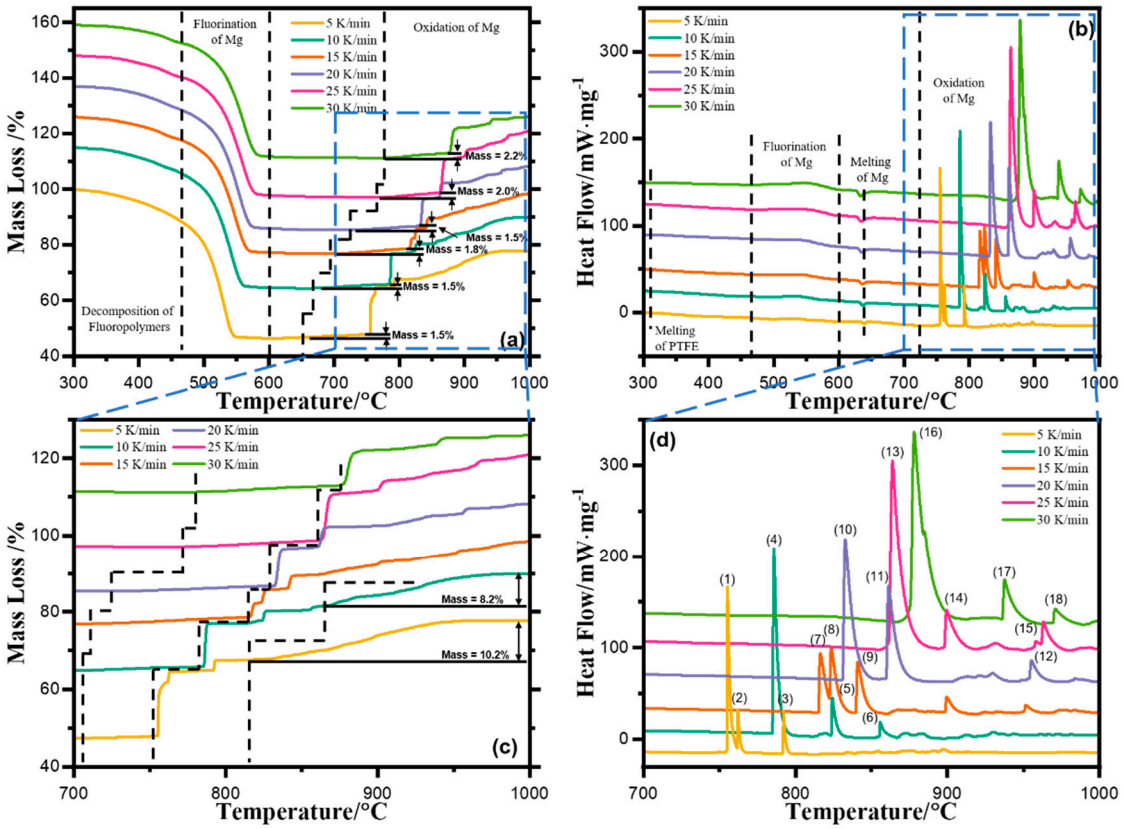

Figure 4. The TG-DSC curves of the oxidation of MTV at 5, 10, 15, 20, 25, and 30 K/min under the atmosphere of O_2. (**a**,**b**) Curves of TG and DSC from 300~1000 °C, respectively; (**c**,**d**) curves of TG and DSC from 700~1000 °C of TG and DSC, respectively. The mass ratio of MTV was 47.6:47.6:4.8.

As depicted in Figure 4a, from 300 to 600 °C, nearly 50% mass losses were observed on the TG curves, where mass increases were observed when the temperature rose above 650 °C. Correspondingly, in Figure 4b, minor exothermic peaks were observed in the DSC curves between 460 and 600 °C, where sharp exothermic peaks were observed when the temperature rose above 650 °C. Furthermore, endothermic peaks were simultaneously observed in the DSC curves. According to previous investigations [13], the mass losses were due to the decomposition of Teflon, and the mass increases were due to the oxidation of Mg. The minor exothermic peaks were due to the fluorination of Mg, and the enormous heat releases were due to the oxidation of Mg.

Therefore, the reaction of MTV in air can be divided into two stages at the temperature of 600 °C. The first stage is the fluorination of Mg with fluoropolymers, and the second stage is the oxidation of the exceeded Mg. Furthermore, the main difference in the oxidation of the exceeded Mg was the onset temperature of the oxidation. First, the mass increase in the oxidation of Mg started at 700 °C, higher than its melting point, resulting in the gas–solid oxidation of Mg. Second, because the end temperature of the oxidation of the exceeded Mg was 950 °C, much higher than that of the oxidation of pure Mg (Figure 1c).

These results suggest that after fluorination, the oxidation of Mg was severely impeded. Since both the oxidation and fluorination of Mg started in the outer layer of the spherical particle, the morphology of the outer layer could be the key to these changing features. Therefore, an ex situ morphology characterization protocol on the reaction products of MTV in air under a designated heating temperature was conducted first via optical microscopy and then by SEM-EDS mapping.

3.5. The Morphology of Oxidation Products of MTV in Air Characterized via Optical Microscope

As depicted in Figure 5, the morphology of the oxidation product of MTV in air could be divided into two kinds: the gray spherical particle and the white irregular particle. At the temperature of 700 °C, the gray spherical particle suggests that the fluorination of Mg can generate MgF_2 and reduce the metallic luster when it does not change the spherical shape. From the temperature of 700 to 800 °C, several particles expanded to a white irregular shape, while the rest of the particles were still gray spherical particles, which suggests that the oxidation of Mg started. Of note, several bubbles were observed on the white particles. This suggests that gaseous Mg was generated as the Mg particles were oxidized. As the temperature rose above 900 °C, all of the particles turned to white and expanded to an irregular shape. Furthermore, numerous diffused white powders were also observed. The generation of diffused white powder suggests that more gaseous Mg was generated at 900 °C.

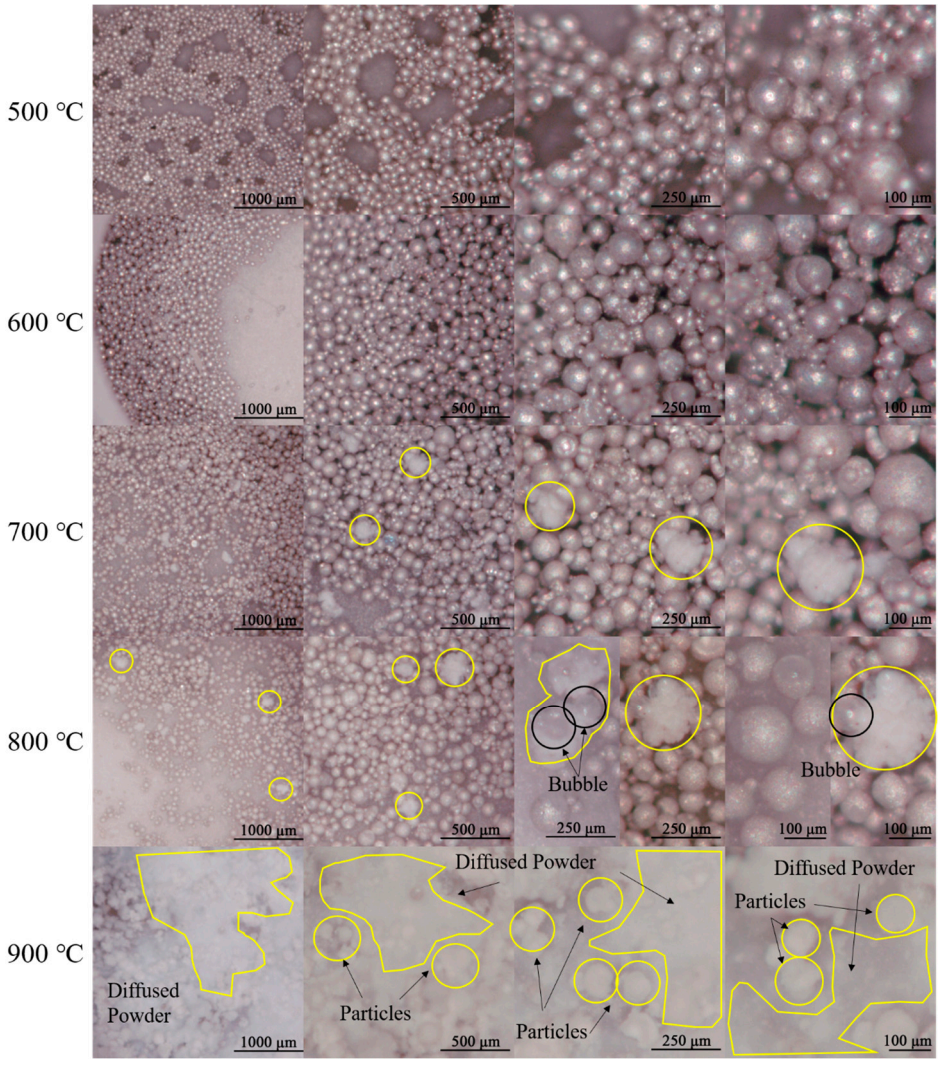

Figure 5. The morphology of the residues of the oxidation of MTV at 500 °C, 600 °C, 700 °C, 800 °C, and 900 °C magnified 50, 100, 200, and 300 times via optical microscopy. The white balance was set as AUTO.

Therefore, the oxidation of the exceeded Mg began and ended at the temperatures of 700 and 900 °C, respectively, 100 and 250 °C higher than those of pure Mg, respectively. It also suggests the prolonged oxidation of the exceeded Mg. Furthermore, the bubble structure and diffused white powders indicated that the oxidation of Mg above 800 °C could be a homogeneous reaction.

3.6. The Morphology of the Oxidation Products of MTV in Air Characterized via SEM-EDS-Mapping

To further investigate the morphology of the oxidation products of MTV in air impediment, FESEM-EDS mapping was conducted on the MTV sample after heating at the designated temperature. The results are shown in Figures 6–8.

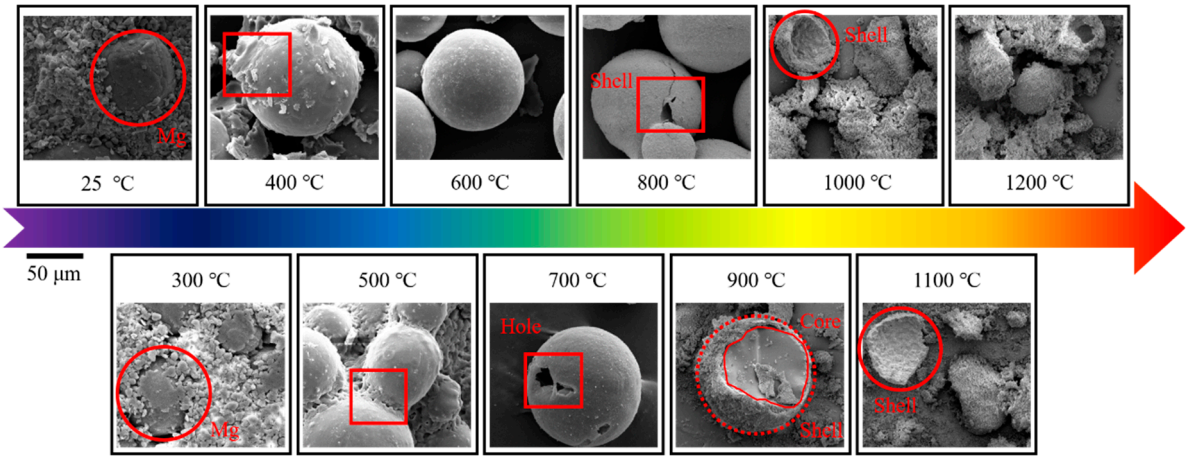

Figure 6. The morphology of the surface of MTV after heating at 300 °C, 400 °C, 500 °C, 600 °C, 700 °C, 800 °C, 900 °C, and 1200 °C in air. The heating rate was 10 K/min. The magnification was 5000 times. The detailed SEM results are depicted in Figures S9–S19.

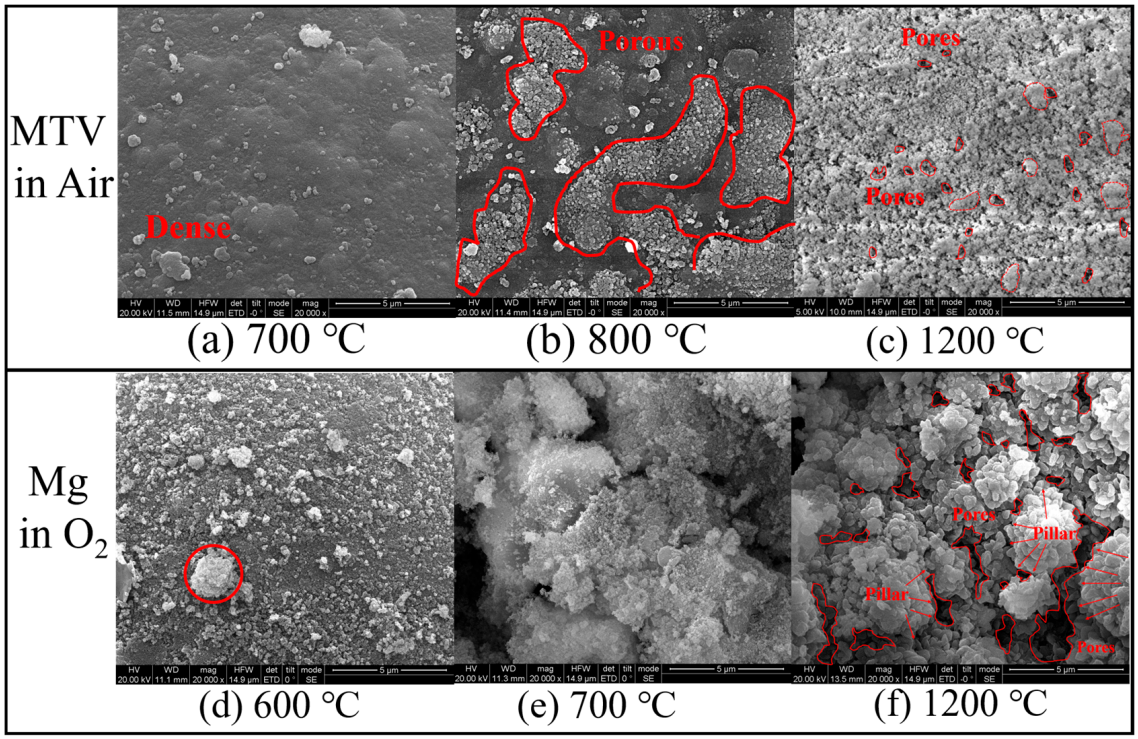

Figure 7. The morphology of the surface of MTV after heating at (**a**) 700 °C, (**b**,**c**) 800 °C, and (**f**) 1200 °C under air and Mg after heating at (**d**) 600 °C and (**e**) 700 °C and (**f**) 1200 °C via SEM. The heating rate was 10 K/min. The magnification was 20,000 times. High resolution version of (**c**,**f**) including the calculation process are presented in Figures S20–S23.

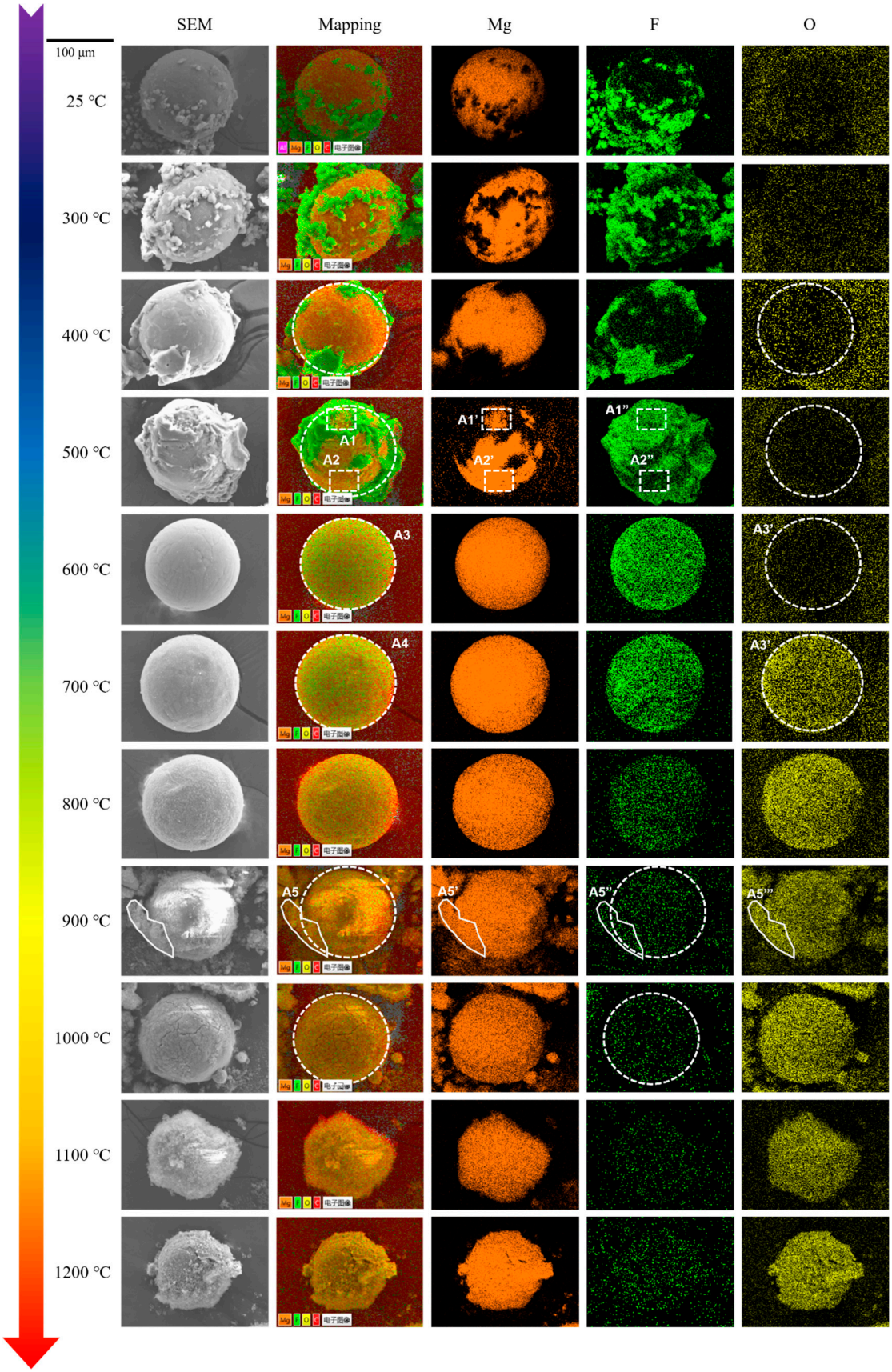

Figure 8. The mapping results of the surface of MTV after heating at 300 °C, 400 °C, 500 °C, 600 °C, 700 °C, 800 °C, 900 °C, and 1200 °C in air. The heating rate was 10 K/min. The magnification was 5000 times.

As illustrated in Figure 6, the morphology of Mg can be concluded as a core-shell structure. By the temperature of 600 °C, the attachment surrounding the sphere was melted Teflon. As the temperature rose to 700 °C, the Teflon completely decomposed, and holes in the spherical Mg were observed. At 800 °C, a core-shell structure was formed, where cracks and a hole were observed in the shell. As the temperature rose to 900 °C, the Mg core was partially consumed, and the shell corrupted, presenting a thickness of a 2.45 μm shell. When the temperature rose to 1200 °C, the Mg core was completely oxidized, and the MgF_2 shell was left.

Therefore, this MgF_2 outer shell could impede the oxidation of Mg, further suggesting the protective feature of this MgF_2 shell. This protective feature of the MgF_2 layer was investigated in 1934, where Reimers listed several gases preventing Mg from burning, which included SF_6. In the 1970s, Fruehling and Hanawalt thoroughly investigated the application of SF_6 as a protective gas, and proposed that a low content of SF_6 in air could sufficiently protect Mg [15]. The protective mechanism was the protective layer of MgF_2, which was first observed in the sodium fluorine solution in 1954. In [16], the fluorine layer for protecting Mg and its alloys was thoroughly reviewed.

To thoroughly compare the morphologies of Mg in O_2 and MTV in air, the partial surface morphology of the two examples after heating at 600, 700, and 1200 °C was depicted, as shown in Figure 7.

As shown in Figure 7, after heating at 700 °C, the surface of Mg was dense, on which a few nodes were separated. As the temperature rose to 800 °C, porous MgO nodes generated on the Mg surface (red circled area). Meanwhile, the rest of the Mg surface was still dense. However, when the heating temperature rose to 1200 °C, the particle surface was completely porous.

On the other hand, the surface of Mg was completely covered by MgO nodes when Mg oxidized at 600 °C, when it was completely porous and shattered at 700 °C. Therefore, the porous morphology of the oxidation of Mg occurred at 700 °C, when that of MTV occurred higher that 800 °C.

Of note, the porous morphologies of these two samples at 1200 °C were different. After MTV reacted in air at 1200 °C, the pores on the surface of MgO appeared to be smaller. The mean value of that was 0.27 μm (Figures 7c, S20 and S21). Furthermore, the porous morphology was flat and continuous. On the other hand, after Mg oxidized at 1200 °C, MgO appeared to be staked upon each other, forming MgO pillars, while the pillar was separated from each other by pores (Figures 7f, S22 and S23). The mean value of these pores was 0.42 μm, 55.5% bigger than that of the MTV sample.

Furthermore, the elemental distributions on the surface of MTV after heating at 300 °C, 400 °C, 500 °C, 600 °C, 700 °C, 800 °C, 900 °C, and 1200 °C in air were investigated. The characteristic results are shown in Figure 8.

From the temperature of 25 to 600 °C, F 1α was first not well-distributed, and gradually separated on the surface of Mg. It suggests that during this period, the fluoropolymers decomposed and fluorine moved from the polymers onto Mg, where the dense MgF_2 shell gradually formed, surrounding the Mg core (Figure S24, [13]). This indicates that the fluorination of Mg is a solid–solid phase reaction.

As the temperature rose from 600 to 1200 °C, F 1α gradually disappeared, while O 1α was gradually generated. The existence of O 1α confirmed that the oxidation of Mg started. The disappearance of F 1α could be due to the generation of MgO over the MgF_2 shell.

To further investigate the changing content of Mg, O, and F in the oxidation of Mg and MTV, respectively, EDS was conducted simultaneously.

As depicted in Figure 9a, due to the slow oxidation process of Mg, its mass fraction only slightly decreased when the temperature reached 600 °C. However, when the temperature rose to 700 °C and higher, the mass fraction of Mg rapidly dropped to 60% and remained consistent, indicating a complete oxidation of Mg. This was further confirmed by the change in the mass fraction of O in the oxidation of Mg, as shown in Figure 9b.

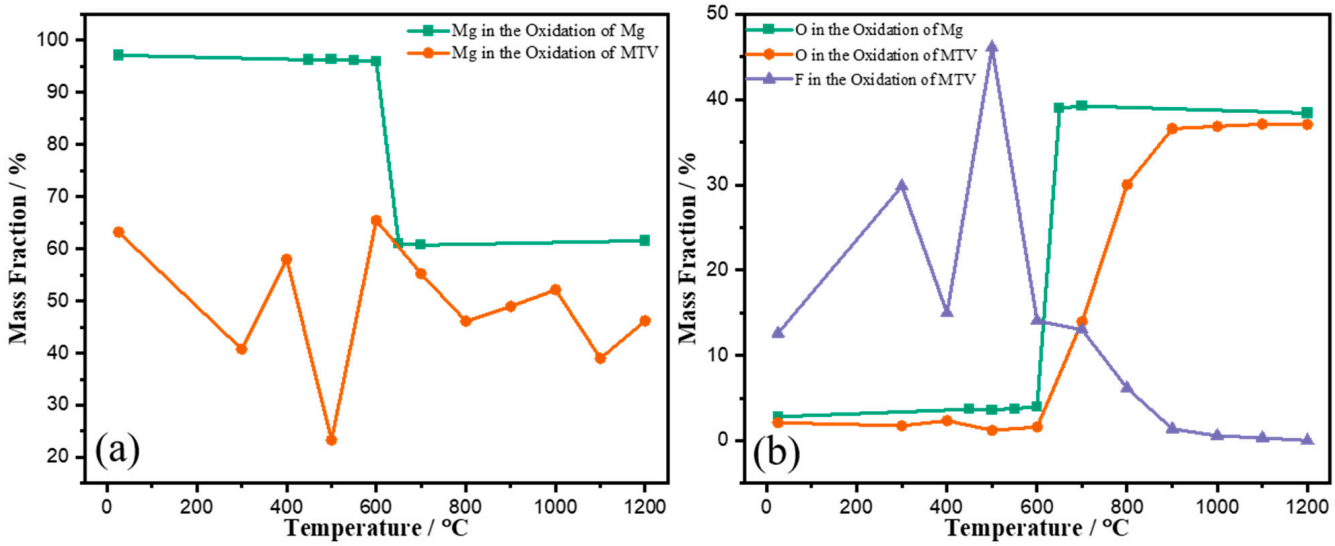

Figure 9. The mass fraction of Mg in Mg and MTV (**a**) and O (F and O) in Mg and MTV (**b**).

On the other hand, when Mg was oxidized in MTV, there was no clear pattern in the changing mass fraction of Mg. When the temperature increased from 600 °C to 1200 °C, the mass fraction of F decreased to 0, while the mass fraction of O increased from 0 to 37%. This was consistent with the mapping results. Furthermore, the rate of increase in O in the oxidation of fluorinated Mg was much lower compared to pure Mg, indicating a prolonged oxidation process of fluorinated Mg.

The SEM-EDS mapping results indicate that after the fluorination of Mg, a dense MgF2 shell was formed that hindered the oxidation of Mg. This led to the oxidation of Mg only starting after melting and vaporization, resulting in a severe homogeneous oxidation.

4. Conclusions

The oxidation of magnesium is rapid and easily noticeable. At temperatures below 550 °C, the magnesium retained its metallic luster. However, at 600 °C, only a few particles turned white and became irregularly shaped. At 650 °C, all of the magnesium particles had oxidized and transformed into porous, irregularly shaped magnesium oxide.

When MTV was exposed to air, the reaction could be divided into two stages at 600 °C. The first stage was the fluorination of magnesium, which formed a dense shell of magnesium fluoride (MgF_2). The dense MgF_2 shell hindered the oxidation of magnesium, causing it to only begin after melting and vaporization, leading to severe homogeneous oxidation.

Supplementary Materials: The following supporting information can be downloaded at: https://www.mdpi.com/article/10.3390/met13020417/s1, Figure S1: The mapping results of the surface of Mg after the heating at 300 °C, 400 °C,500 °C, 600 °C, 700 °C and 1200 °C in O_2. The heating rate was 10 K/min. The magnification was 5000 times; Figure S2: The SEM results of the surface of Mg at 25 °C; Figure S3: The SEM results of the surface of Mg after the heating at 500 °C in O_2; Figure S4: The SEM results of the surface of Mg after the heating at 550 °C in O_2; Figure S5: The SEM results of the surface of Mg after the heating at 600 °C in O_2; Figure S6: The SEM results of the surface of Mg after the heating at 650 °C in O_2; Figure S7: The SEM results of the surface of Mg after the heating at 700 °C in O_2; Figure S8: The SEM results of the surface of Mg after the heating at 1200 °C in O_2; Figure S9: The SEM results of the surface of MTV at 25 °C; Figure S10: The SEM results of the surface of MTV after the heating at 300 °C in air; Figure S11: The SEM results of the surface of MTV after the heating at 400 °C in air; Figure S12: The SEM results of the surface of MTV after the heating at 500 °C in air; Figure S13: The SEM results of the surface of MTV after the heating at 600 °C in air; Figure S14: The SEM results of the surface of MTV after the heating at 700 °C in air; Figure S15: The SEM results of the surface of MTV after the heating at 800 °C in air; Figure S16: The SEM results of the surface of MTV after the heating at 900 °C in air; Figure S17: The SEM results of the surface of MTV after

the heating at 1000 °C in air; Figure S18: The SEM results of the surface of MTV after the heating at 1100 °C in air; Figure S19: The SEM results of the surface of MTV after the heating at 1200 °C in air; Figure S20: The calculation area of Nanometer 1.2 on the surface of MTV after the heating at 1200 °C in air; Figure S21: The calculation report of Nanometer 1.2 on the surface of MTV after the heating at 1200 °C in air; Figure S22: The calculation area of Nanometer 1.2 on the surface of Mg after oxidizing at 1200 °C in O_2; Figure S23: The calculation area of Nanometer 1.2 on the surface of Mg after oxidizing at 1200 °C in O_2; Figure S24: The XRD results of the residues of MTV after calcinated at 600, 700 and 1000 °C [1] in air, respectively.

Author Contributions: Conceptualization, Y.L. (Yifan Li); methodology, Y.L. (Yifan Li).; formal analysis, Y.L. (Yifan Li); investigation, Y.L. (Yifan Li); data curation, J.W., H.L.; writing—original draft preparation, Y.L. (Yifan Li); writing—review and editing, D.S. (Dong Shen); supervision, D.S. (Dongming Song); project administration, Y.L. (Yanchun Li). All authors have read and agreed to the published version of the manuscript.

Funding: This research received no funding.

Institutional Review Board Statement: Not applicable.

Informed Consent Statement: Not applicable.

Data Availability Statement: Data sharing is not applicable to this article.

Conflicts of Interest: The authors declare no conflict of interest.

References

1. Coffin, K. Burning Times of Magnesium Ribbons in Various Atmospheres, No. NACA-TN-3332. 1954. Available online: https://ntrs.nasa.gov/citations/19930084125 (accessed on 13 February 2023).
2. Markstein, G. Magnesium-oxygen dilute diffusion flame. In *Symposium (International) on Combustion*; Elsevier: Amsterdam, The Netherlands, 1963; pp. 137–147. [CrossRef]
3. Ozerov, E.; Skvortsov, I. Combustion of a conglomerate of magnesium particles. *Combust. Explos. Shock Waves* **1971**, *7*, 191–194. [CrossRef]
4. Moser, G.; Tschamber, V.; Schonnenbeck, C.; Brillard, A.; Brilhac, J.-F. Kinetic Analysis and Modelling of Mg Powder Slow Combustion. In Proceedings of the 3rd World Congress on Momentum, Heat and Mass Transfer, Budapest, Hungary, 12–14 April 2018. [CrossRef]
5. Shafirovich, E.; Goldshleger, U. Combustion of magnesium particles in carbon dioxide and monoxide. In Proceedings of the 31st Joint Propulsion Conference and Exhibit, San Diego, CA, USA, 10–12 July 1995. [CrossRef]
6. Moser, G.; Tschamber, V.; Schönnenbeck, C.; Brillard, A.; Brilhac, J.-F. Non-isothermal oxidation and kinetic analysis of pure magnesium powder. *J. Therm. Anal. Calorim.* **2018**, *136*, 2145–2155. [CrossRef]
7. Moser, G.; Schönnenbeck, C.; Tschamber, V.; Brillard, A.; Brilhac, J.-F. Experimentation and kinetic modeling of low-temperature oxidation of magnesium particles for the production of energy with low environmental impact. *Combust. Flame* **2021**, *230*, 111419. [CrossRef]
8. Kim, Y.; Yim, C.; Kim, H.; You, B. Key factor influencing the ignition resistance of magnesium alloys at elevated temperatures. *Scr. Mater.* **2011**, *65*, 958–961. [CrossRef]
9. Baubekova, G.; Akilbekov, A.; Kotomin, E.A.; Kuzovkov, V.N.; Popov, A.I.; Shablonin, E.; Lushchik, A. Thermal annealing of radiation damage produced by swift 132Xe ions in MgO single crystals. *Nucl. Instrum. Methods Phys. Res. Sect. B Beam Interact. Mater. At.* **2019**, *462*, 163–168. [CrossRef]
10. Popov, A.I.; Elsts, E.; Kotomin, E.A.; Moskina, A.; Karipbayev, Z.T.; Makarenko, I.; Kuzovkov, V.K. Thermal annealing of radiation defects in MgF2 single crystals induced by neutrons at low temperatures. *Nucl. Instrum. Methods Phys. Res. Sect. B Beam Interact. Mater. At.* **2020**, *480*, 16–21. [CrossRef]
11. Nakamura, F.; Kato, T.; Okada, G.; Kawaguchi, N.; Fukuda, K.; Yanagida, T. Scintillation, TSL and RPL properties of MgF2 transparent ceramic and single crystal. *Ceram. Int.* **2017**, *43*, 7211–7215. [CrossRef]
12. Pourmortazavi, S.; Babaee, S.; Ashtiani, F. Statistical optimization of microencapsulation process for coating of magnesium particles with Viton polymer. *Appl. Surf. Sci.* **2015**, *349*, 817–825. [CrossRef]
13. Li, Y.; Wang, J.; Liu, H. Combustion properties of Mg-based ignition charge using Mg-Gd alloy powder as the fuel. *Chem. Eng. J.* **2022**, *441*, 135633. [CrossRef]
14. Shevtsov, V.; Fursov, V.; Stesik, L. Mechanism for combustion of isolated magnesium particles. *Combust. Explos. Shock Waves* **1976**, *12*, 758–763. [CrossRef]

15. Fruehling, J. Protective Atmospheres for Molten Magnesium, University of Michigan. 1970. Available online: https://www.proquest.com/openview/1da664ceb95df7aef0cbc1e51a5e07ff/1?pq-origsite=gscholar&cbl=18750&diss=y (accessed on 13 February 2023).
16. Yamaguchi, S. Protective Films on Magnesium Observed by Electron Diffraction and Microscopy. *J. Appl. Phys.* **1954**, *25*, 1437–1438. [CrossRef]